

NJC

Accepted Manuscript



This article can be cited before page numbers have been issued, to do this please use: Y. Zhang, J. Wang, Y. Wei and X. Zhang, *New J. Chem.*, 2017, DOI: 10.1039/C6NJ03414D.



This is an Accepted Manuscript, which has been through the Royal Society of Chemistry peer review process and has been accepted for publication.

Accepted Manuscripts are published online shortly after acceptance, before technical editing, formatting and proof reading. Using this free service, authors can make their results available to the community, in citable form, before we publish the edited article. We will replace this Accepted Manuscript with the edited and formatted Advance Article as soon as it is available.

You can find more information about Accepted Manuscripts in the [author guidelines](#).

Please note that technical editing may introduce minor changes to the text and/or graphics, which may alter content. The journal's standard [Terms & Conditions](#) and the ethical guidelines, outlined in our [author and reviewer resource centre](#), still apply. In no event shall the Royal Society of Chemistry be held responsible for any errors or omissions in this Accepted Manuscript or any consequences arising from the use of any information it contains.



Journal Name

ARTICLE

Robust Urethane-Bridged Silica Aerogels Available for Water-Carved Aerosculptures

Yulu Zhang[†], Jin Wang[†], Yong Wei and Xuotong Zhang^{*}

Received 00th January 20xx,
Accepted 00th January 20xx

DOI: 10.1039/x0xx00000x

www.rsc.org/

Molecular bridged silica aerogels have received extensive interests in recent years due to their easily controlled mechanical properties varied with different organosilane precursors, and without any further post-modification. In this work, a series of novel and robust molecular bridged silica aerogels were prepared by using a symmetrical urethane-bridged monomer, named N, N-bis(propyltriethoxysilyl)carbamide (bPTSCA), which was synthesized via a solvent-free exothermic reaction between 3-Isocyanatopropyltriethoxysilane (IPTES) and 3-Aminopropyltriethoxysilane (APTES) in several minutes at normal temperature and pressure. The influence of catalysts on the obtained gels and aerogels were studied in detail. It was found that NH₄F aqueous solution showed the most effective catalysis capability, and the corresponding aerogels were intact with slight shrinkages. The mechanical strength of these aerogels could reach as high as 100 times more than that of the native silica aerogels (unbridged), and the strength could be easily adjusted from rigid region to elastic region simply by varying the sample density. Moreover, these aerogels possessed an interesting character of regional shrinking when encountering with water, which made it possible to fabricate artistic aerosculptures with water or other polar solvents as graver.

Introduction

Aerogels, known as frozen smoke or air-glass, are a special class of highly porous materials derived from gels by exchanging the pore liquids with air while maintaining the network structure as the original gels.¹⁻⁵ Due to their exceptional properties such as low density, high porosity and large specific surface area, silica aerogels are of great interest in a wide variety of applications including thermal insulation,^{6,7} sound/gas absorption,^{8,9} nonlinear optical response,^{10,11} water remediation,¹²⁻¹⁴ drug delivery,¹⁵⁻¹⁷ catalysis supports,^{18, 19} energy storage,^{20, 21} and even for cosmic dust capture.²² However, there exists a wide disparity between their theoretical and actual applications since silica aerogels are inherently fragile.^{1, 23} Therefore, great efforts have been devoted to strengthening the gel network, and the commonly used mechanism is to reinforce the interparticle necks which are the weak points of the aerogel skeletal framework.²⁴ The most straightforward way is to increase the density^{25, 26} or prolonging the aging time of the preliminary gels,^{27, 28} whereas the final improvement in mechanical property is quite limited. Another approach to strengthen silica aerogels is to impregnate or disperse individual micro/nanoscope secondary

phase, such as polymers^{29, 30} or fibers,^{31, 32} into the silica matrix, thus the obtained hybrid aerogels are deservedly heterogeneous at the molecular level. Besides, chemical crosslinking with reactive molecules or polymers achieves the most significant improvement in the mechanical properties,³³⁻³⁵ nevertheless this scheme always involves complex synthetic processes and less desirable solvents.

Bridged polysilsesquioxanes are a family of hybrid organic-inorganic materials prepared in a single step from molecular precursors.³⁶ These precursors often contain a variable organic bridging group and two or more trifunctional silyl groups, hence integrate organic and inorganic groups homogeneously at molecular length scales in the ultimate polysilsesquioxanes. Moreover, the bridging organic group allows synthesis of the final products with broad chemical, physical and mechanical properties.^{23, 37} However, compared to their thermal stability, the mechanical properties of bridged polysilsesquioxanes have drawn less attention. In the limited number of reports, ethane-,³⁸ phenylene-,³⁹ hexalene-,⁴⁰ thioether-^{41, 42} and even thiourethane-bridged⁴³ groups could endow the corresponding polysilsesquioxane materials with improved mechanical properties in different extent. These bridged monomers were always synthesized via special reactions in two or more steps. Herein, we reported a robust silica aerogel derived from urethane-bridged monomer which was synthesized via a one-step solvent-free reaction. It is notable that in the successive hydrolysis and condensation reactions, there was also without any toxic solvent except a common ethanol. In order to investigate the influence of catalyst type to the obtained gels and aerogels, ammonia

^{*}Suzhou Institute of Nano-Tech and Nano-Bionics (SINANO), Chinese Academy of Sciences, Suzhou, 215123, P. R. China, e-mail: zhangxtchina@yahoo.com (X. Zhang)

[†]These authors contribute equally

Electronic Supplementary Information (ESI) available: [the pictures of real product bPTSCA and gels, TEM images, the carving process with hexane]. See DOI: 10.1039/x0xx00000x

ARTICLE

Journal Name

hydroxide, hydrochloric acid and ammonium fluoride were separately used as catalyst, and coupled with different monomer densities and molar ratios of water to Si ($\text{H}_2\text{O}:\text{Si}$). It was found that the physical properties of the final silica aerogels varied with the catalyst type, and particularly their mechanical properties ranged from rigidity to elasticity along with the decreased monomer density.

In addition, the artistic worthiness of aerogels was captured by Greek visual artist I. Mechaloudis, and the first aerosculpture was realized with an aesthetic view in 2002.⁴⁴ Thereafter, few reports were devoted on this topic, since it is quite unusual that this scientific and technological aerogel material is applied in art area. Herein, we would discuss a relative application in a scientific view, inspired by an interesting phenomenon that these urethane-bridged silica aerogels would regionally shrink when they are encountering with water. In another word, aerosculptures could be created on these urethane-bridged silica aerogels, applied water as gravers.

Experimental section

Materials

All solvents and reagents were used as received from each manufacturer. 3-Aminopropyltriethoxysilane (APTES, $\geq 99\%$), 3-Isocyanatopropyltriethoxysilane (IPTES, $\geq 95\%$) and Rhodamine B ($\geq 95\%$, HPLC) were purchased from the Aladdin Industrial Corporation (Shanghai, China). Anhydrous ethanol (EtOH, $\geq 99.7\%$), ammonia hydroxide ($\text{NH}_3\cdot\text{H}_2\text{O}$, 25%-28% by weight), hydrochloric acid (HCl aqueous solution, 36%-38%) and ammonium fluoride (NH_4F , 99%) were all obtained from Sinopharm Chemical Reagent Co. Ltd (Shanghai, China).

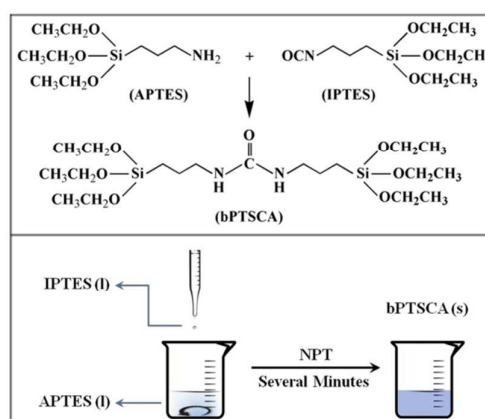
Synthesis of N, N-bis(propyltriethoxysilyl)carbamide (bPTSCA)

As shown in Scheme 1, IPTES were added dropwise into APTES under vigorous stirring, maintaining the final molar ratio of IPTES: APTES = 1:1. After a successive stirring and continual heat release for several minutes, the mixture liquid of IPTES and APTES abruptly turned to a gray-white solid with a constant volume (seen in Fig. S1). This gray-white solid would be used as monomer in the next sol-gel process. Yield: $\geq 99\%$. ^1H NMR (DMSO, 400 MHz, ppm): $\delta = 5.76$ (2H, t, N-H), 3.72 (12H, q, O-CH₂-C), 2.92 (4H, q, N-CH₂-C), 1.37 (4H, m, C-CH₂-C), 1.12 (24H, t, CH₃), 0.48 (4H, t, C-CH₂-Si).

Preparation of urethane-bridged silica gels and aerogels

Urethane-bridged silica gels were prepared via sol-gel process, using the common and nontoxic ethanol as the only solvent. 1M HCl aqueous solution and 1M NH_4F aqueous solution were separately prepared in advance, and got ready to be applied as catalyst, as well as the original ammonia hydroxide. For a typical process, 468 mg (1 mmol) bPTSCA was taken and dissolved in 4.8 ml EtOH to obtain a colorless and clear

solution; then 200 μl 1M HCl aqueous solution was added in the above solution under stirring; after successive stirring for about 1 min, a sol gradually formed and stood still to further establish a corresponding gel. After a three-days aging time, the gel undergone solvent exchange process with EtOH for another three days, to replace the water taken by the catalyst or generated by the condensation reaction; then a supercritical drying process with CO_2 (10 MPa, 40°C) was carried out on the gel, and finally a urethane-bridged silica aerogel formed.



Scheme 1 Schematic diagram of synthesis reaction and process for bPTSCA

Creation of aerosculptures with water as graver

To carve an intact bulk of aerogel, water or other polar liquid (such as EtOH) could be used as graver. Herein, printing with assistant of empastic signets was chosen to reveal the carving effect. In carving process, a proper amount of water was homogeneously coated on the pattern of a signet; then the coated signet came into contact with the aerogel bulk for several seconds; and finally, intagliated pattern was leaved after withdrawing the signet. In order to make the nicks distinct, the water used as inkpad was dyed with Rhodamine B.

Characterization

The ^1H NMR spectra were detected on a VNMRS 400 MHz spectrometer (Varian, Inc., Palo Alto, CA), with DMSO- d_6 as solvent. The Fourier transform infrared (FTIR) spectra were measured on a Nicolet iN10 spectrometer (Thermo Scientific, USA) using a reflection mode. The surface areas of the aerogels were determined via the Brunauer-Emmett-Teller (BET) method (ASAP 2020, Micromeritics, USA) based on the amount of N_2 adsorbed at pressures $0.05 < P/P_0 < 0.3$; the cumulative pore volume was measured at the point $P/P_0 = 0.99$; the pore size distribution and the average pore diameters were analyzed by the BJH (Barrett-Joyner-Halenda) method. The samples for microscopy were coated with Au nano-powder at a current of 20 mA for 2 min, and then viewed using a S4800 field-emission scanning electron microscopy

(FESEM, Hitachi, Japan). The densities of the aerogels bulk were calculated from their measured weight and volume. The mechanical properties of aerogel samples were evaluated on an Instron 3365 universal test machine (Instron Corp., Norwood, USA) using a compress and release routine and/or unidirectional compression mode.

Results and discussion

Synthesis and characterization of bPTSCA

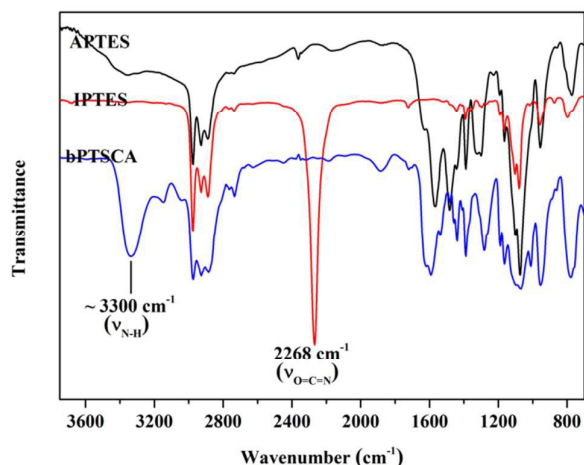


Fig. 1 FTIR spectra of APTES, IPTES and bPTSCA

Isocyanates and amines are the most frequently used starting materials for preparing bridged monomers. Isocyanates could react readily with amines to give urea linkages. However, few studies were devoted on urethane-bridged monomers and their derived polysilsesquioxanes. Herein, a symmetrical monomer, named N, N-bis(propyltriethoxysilyl)carbamide (bPTSCA), was designed and expected to be obtained via a simple solvent-free exothermic reaction between APTES and IPTES. The FTIR and ^1H NMR spectra for APTES, IPTES and their reaction product were shown in Fig. 1 and Fig. 2 respectively. In the FTIR spectra, the asymmetry stretching vibration peak of isocyanate groups ($-\text{N}=\text{C}=\text{O}$) at 2268 cm^{-1} is absent in the spectrum of the product, indicating the isocyanate groups in IPTES have been completely consumed. In addition, the broad adsorption band around 3300 cm^{-1} corresponding to the vibration of N-H in APTES have turned into a sharp band after the reaction, reckoned as a characteristic peak for N-H in amide groups. According to the ^1H NMR spectra, the chemical shifts of protons in APTES appeared at 3.73 ppm (a2), 3.43 ppm (a5), 1.36 ppm (a6), 1.12 ppm (a1), 1.04 ppm (a4) and 0.52 ppm (a3); in IPTES at 3.75 ppm (b2), 3.30 ppm (b5), 1.58 ppm (b4), 1.13 ppm (b1) and 0.58 ppm (b3). Upon the reaction between these two raw materials, the protons in $-\text{NH}_2$ (a6 at 1.36 ppm) disappeared, and a new resonance band appeared

at 5.76 ppm (c6) assigned to the protons in the newly generated urea group linkage ($-\text{NHCONH}-$). These coupled FTIR and ^1H NMR spectra demonstrated the successful synthesis of bPTSCA, and furthermore, illustrated that the $-\text{NCO}$ and $-\text{NH}_2$ were mostly consumed and the reaction presented a high conversion. Consequently, this synthesized urethane-bridged monomer would be used as obtained in the next sol-gel process without any further purification.

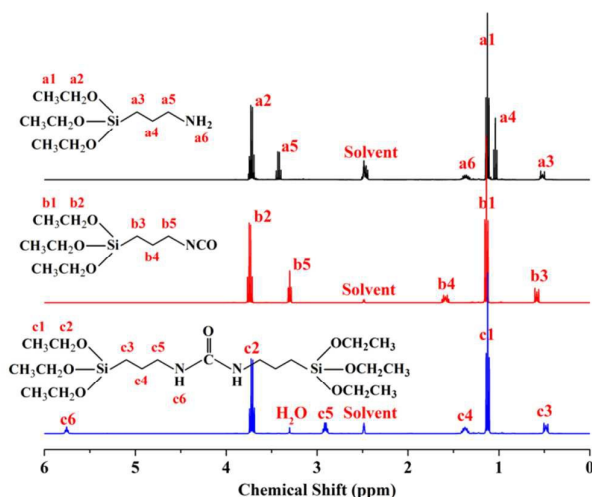


Fig. 2 ^1H NMR spectra of APTES, IPTES and bPTSCA

Influence of catalyst type to gels

The excellent performances of aerogels are all originated from the gels. Therefore, selecting gels with favorable characters is a vital issue in preparation of aerogels. In this work, ammonia hydroxide (25%-28% by weight), 1 M HCl aqueous solution and 1 M NH_4F aqueous solution were separately used as catalyst in the sol-gel process. When assigned a same catalyst density for samples shown in Table 1, the varied gelation time appeared much dependent on the catalyst type and the monomer density, and indicated that NH_4F was the most efficient catalyst, while ammonia hydroxide was the lowest one. This could be explained as follows based on the sol-gel mechanism of siloxane proposed by C. J. Brinker and G. W. Scherer.⁴⁵ In the hydrolysis reaction of urethane-bridged bPTSCA, the adjacent electron-donating alkyl chain lowered the base-catalyzed hydrolysis rate, while improved the acid-catalyzed rate; in addition, the speed of condensation catalyzed by acid is inherently faster than that catalyzed by base. Consequently, the samples catalyzed by ammonia hydroxide consumed longer time to finish the gel process. In terms of appearance (as seen in Fig. S2), all the gels (AH1-AH4) catalyzed by ammonia hydroxide were transparent with a light blue color, whereas the transparent gels only formed at high monomer density when catalyzed by HCl or NH_4F . However, it was found that in the two series of HA and AF, high monomer density (generally $\geq 0.6\text{ mol/L}$ for Sample HA and $\geq 0.7\text{ mol/L}$ for Sample AF) would result in obvious syneresis and crack (as the insets

ARTICLE

Journal Name

shown in Fig. S2). It was reckoned that the samples with ultra-high density catalyzed by HCl or NH_4F , turned into gels at a low reaction degree of condensation; once gels formed, condensation reaction continued, hence abundant covalent bonds jointed, and thus contracted the framework of gels to shrink. While shrinkage occurred, certain amount of solvent EtOH (including some slight water) extruded; therefore some menisci emerged in the mesopores, produced nonuniform capillary forces, and finally lead to crack in gels. Fortunately, the higher reaction degree before gelling kept the samples with lower density away from these shrinkage and crack.

Table 1 Recipe and appearance of the gels and their corresponding aerogels catalyzed by different catalyst

Sample	C_{Monomer}^d (mol/L)	Gelation Time	Gel Appearance	Aerogel Appearance
AH1 ^a	0.1	~ 24 h	transparent	collapse
AH2 ^a	0.2	~ 24 h	transparent	collapse
AH3 ^a	0.4	~ 24 h	transparent	collapse
AH4 ^a	0.6	~ 48 h	transparent	collapse
HA1 ^b	0.1	- ^e	-	-
HA2 ^b	0.2	~ 20 min	white	white, intact
HA3 ^b	0.4	~ 20 min	translucent	white, intact
HA4 ^b	0.5	~ 20 min	translucent	white, intact
AF1 ^c	0.1	~ 10 min	white	white, intact
AF2 ^c	0.2	~ 10 min	white	white, intact
AF3 ^c	0.4	~ 10 min	white	white, intact
AF4 ^c	0.6	~ 10 min	white	white, crack

Note: a. Samples catalyzed by ammonia hydroxide (AH); b. Samples catalyzed by 1 M HCl aqueous solution (HA); c. Samples catalyzed by 1 M NH_4F aqueous solution (AF); d. the concentration of bPTSCA; e. precipitation occurred in Sample HA1 after standing still for about 3 h.

Influence of catalyst type to aerogel

After supercritical drying with CO_2 , all gels turned into white aerogels with different degrees of shrinkage. The appearance of these aerogels was described in Table 1 and their density was shown in Table 2. It was found that the shrinkage of samples catalyzed by NH_4F , was the smallest among the three series of samples, while those catalyzed by $\text{NH}_3\cdot\text{H}_2\text{O}$ appeared drastic shrinkage and crack. Considering the same drying process, this discrepancy might be caused by the variable inherent characters of the wet gels, probably as stated above that the condensation degree, before gelling or drying, was the key. As known, the reaction rate of condensation catalyzed by base is much slower than that of acid, while the catalysis efficiency of NH_4F to the same reaction is admitted as higher than common acid.⁴⁵ Consequently, upon the same aging time, gel samples catalyzed by NH_4F possessed a higher condensation degree, and thus a more stable framework to sustain their body weight and if any, the interior stress during drying process. Therefore, the intact aerogels (HA2-HA4 and AF1-AF4) would be the main research objects in the following work.

Physical characters of urethane-bridged silica aerogels

The N_2 adsorption-desorption isotherms of urethane-bridged silica aerogels were shown in Fig. 3. These isotherms exhibited type IV(a) and hysteresis loop H1 according to the IUPAC classification, illustrating the compact of approximately spherical particles arranged in a fairly uniform way,⁴⁶ roughly consistent with the SEM images in Fig. 4. The specific surface areas of these aerogels were evaluated by the Brunauer-Emmett-Teller (BET) method. When HCl aqueous solution was applied as catalyst, the surface area ranged from 150-300 m^2/g , but varied in an irregular way along with the increased density, as well as their pore volume and pore size. However, the surface areas of Sample AF1-AF4 showed a good relationship with monomer density, and particularly Sample AF1 possessed the lowest density but highest surface area and pore volume. Compared to the traditional silica aerogels, however, the surface areas of these urethane-bridged silica aerogels were drastically small, probably due to the blocking effect of urethane-chains to the pores inside the organic-inorganic hybrid aerogel particles.

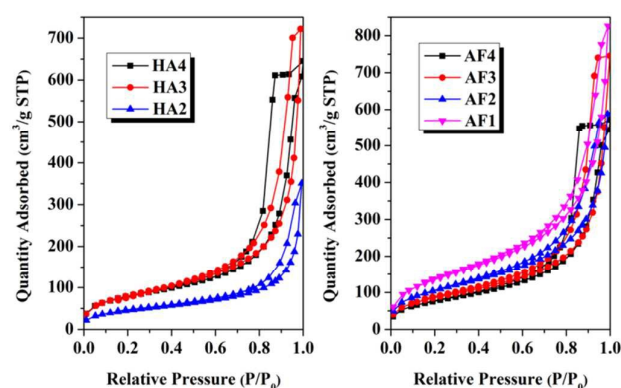


Fig. 3 Nitrogen adsorption and desorption isotherms of urethane-bridged silica aerogels of HA2-HA4 and AF1-AF4

Table 2 Physical properties of the urethane-bridged silica aerogels

Sample	Density (mg/cm^3)	S^a (m^2/g)	V^b (cm^3/g)	D^c (nm)	Modulus E (MPa)
HA2	113	157	0.54	13.35	1.5
HA3	248	280	1.12	15.32	5.9
HA4	430	271	0.99	14.25	21
AF1	49	472	1.28	10.39	0.028
AF2	151	369	0.91	9.47	0.38
AF3	266	299	1.15	14.84	13
AF4	591	268	0.89	12.70	34

Note: a. BET specific surface area of silica aerogels; b. Pore volume of silica aerogels; c. Pore diameter of silica aerogels.

The SEM images in Fig. 4 revealed the morphology of urethane-bridged silica aerogels. As shown, all skeletons of these aerogels were composed of nano-particles with radius ranged from 20 to 50 nm, depending on their density and catalyst used, which could be confirmed more clearly by TEM images in Fig. S3. Interestingly, the particles in HA2 and AF1 “fused” as cakes, very different from those distinct particles in high density samples. This type of fused particles was conjectured to be beneficial to sustain the framework with low density in this work. Moreover, macropores grew along with the decreased bulk density (in another words, the type transformation of particles), indicating different mechanical properties among these aerogel samples.

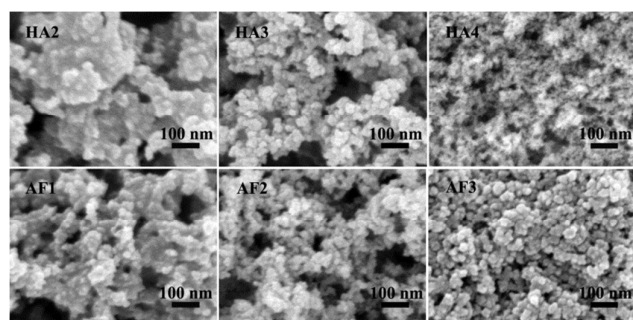


Fig. 4 SEM images of urethane-bridged silica aerogels of HA2-HA4 and AF1-AF3

Fig. 5 showed the stress-strain curves of Sample HA2-HA4 and AF1-AF4, and their Young's Modulus (E) were summarized in Table 2. As seen, the modulus for these two series of samples was almost equaled at similar density. The fragile nature of native silica aerogels have long rendered them unsuitable for load bearing applications. For instance, a native silica aerogel synthesized from TMOS can be completely crushed with the stress of about 31 kPa.⁴⁷ In our work, the maximum stress for urethane-bridged aerogels reached as high as 4 MPa, about 100 times higher than that of the native silica aerogel. Furthermore, their Young's modulus increased with the increase of bulk density, and reached 34 MPa for Sample AF4, as high as 100 fold to that of a native silica whose Young's modulus is about 0.3 MPa.⁴⁰ It was notable that in the wake of the decreased density, samples transformed from rigidity to elasticity. According to the stress-strain curves, Sample HA2 could endure up to 30% linear compression and then spring back to more than 95% of their original size, while Sample AF1 even up to 50%. These urethane-bridged silica aerogels with improved and adjustable mechanical properties could be excellent candidates for more applications.

Application for water-carved aerosculptures

In the measurement of contact angle for these urethane-bridged silica aerogels, it was found that the water dropped on the surface of aerogels gradually permeated into their bodies, and meanwhile left a track in the form of regional shrinkage or

collapse. Inspired by this interesting phenomenon, urethane-bridged silica aerogels could be sculpted to be aerosculptures using water as graver. In this paper, we presented this idea via printing process, and some specimens were exhibited in Fig. 6. The shrinkage nicks were apparent, and maintained intact on samples with high density (e. g., “S” and “A”), whereas cracked to partly fall off on samples with low density. Notably, some other polar solvents, such as EtOH, also worked to obtain similar carved specimens, whereas nonpolar solvents like hexane couldn't (as seen in Fig. S4). As to the reason for this phenomenon, water (or other polar solvents) would develop hydrogen bonding with NH, C=O and OH groups when contacting with urethane-bridged silica aerogels in this work, thus ship inside the nano-pores quickly; along with the spread and evaporation of the shipped water, some meniscuses form, and rouse capillary forces developing against the pores, and finally lead to regional structural collapse.

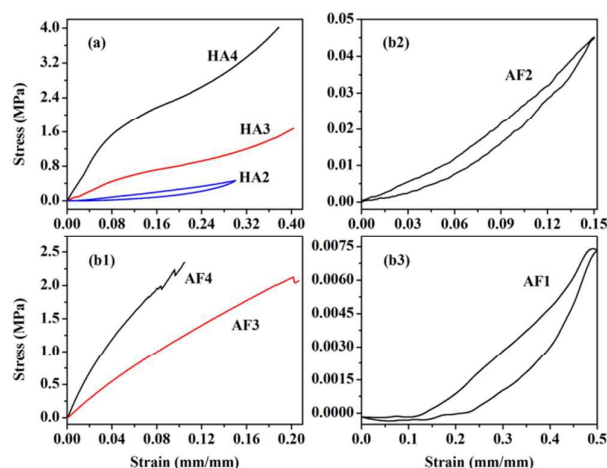


Fig. 5 Stress-Strain spectra of urethane-bridged silica aerogels of HA2-HA4 and AF1-AF3



Fig. 6 Specimens of water-carved urethane-bridged silica aerogels

Conclusions

In this work, urethane-bridged silica aerogels were prepared via a one-step sol-gel process using N, N-bis(propyltriethoxysilyl)carbamide as monomer. This molecular symmetric monomer were designed and successfully synthesized through a solvent-free exothermic reaction between 3-Isocyanatopropyltriethoxysilane and 3-Aminopropyltriethoxysilane, much more easily accessible than other bridged silsesquioxanes. The characters of the obtained gels and aerogels were drastically influenced by the type of catalyst, and intact aerogels could be obtained by the catalysis of HCl aqueous solution and NH₄F aqueous solution, simultaneously with acceptable extent of shrinkage. These urethane-bridged silica aerogels possessed adjustable mechanical properties ranged from rigidity to elasticity according to their density, greatly expanding the application areas of traditional silica aerogels. Moreover, their interesting character of regional shrinking when encountering with water, inspired a new water-carving method for processing aerosculptures, which might be useful in specific areas where special shaped aerogels were needed.

Acknowledgements

This work was financially supported by the National Key Research and Development Program of China (2016YFA0203301), the National Natural Science Foundation of China (51572285, 21373024, 21404117) and the Natural Science Foundation of Jiangsu Province (BK20151234).

Notes and references

- N. Hüsing and U. Schubert, *Angew. Chem. Int. Ed.*, 1998, **37**, 22.
- R. Takahashi, K. Nakanishi and N. Soga, *J. Sol-Gel Sci. and Technol.*, 1997, **8**, 71.
- C. N. Chervin, B. J. Clapsaddle, H. W. Chiu, A. E. Gash, J. H. Satcher and S. M. Kauzlarich, *Chem. Mater.*, 2005, **17**, 3345.
- H. Schäfer, S. Brandt, B. Milow, S. Ichilmann, M. Steinhart and L. Ratke, *Chem. Asian J.*, 2013, **8**, 2211.
- H. Schäfer, B. Milow and L. Ratke, *RSC Adv.*, 2013, **3**, 15263.
- S. Zhao, Z. Zhang, G. Sèbe, R. Wu, R. V. R. Virtudazo, P. Tingaut and M. M. Koebel, *Adv. Funct. Mater.*, 2015, **25**, 2326.
- S. Zhao, W. J. Malfait, A. Demilecamps, Y. Zhang, S. Brunner, L. Huber, P. Tingaut, A. Rigacci, T. Budtova and M. M. Koebel, *Angew. Chem.*, 2015, **127**, 14490.
- G. Rother, L. Vlcek, M. S. Gruszkiewicz, A. A. Chialvo, L. M. Anovitz, J. L. Banuelos, D. Wallacher, N. Grimm and D. R. Cole, *J. Phys. Chem. C*, 2014, **118**, 15525.
- S. Motahari, H. Javadi and A. Motahari, *J. Mater. Civ. Eng.*, 2014, 10.1061/(ASCE)MT.1943-5533.0001208.
- S. Gentilini, F. Ghajeri, N. Ghofraniha, A Di Falco and C. Cnoti, *Optics Express*, 2014, **22**, 1667.
- M. Tabata, I. Adachi, Y. Hatakeyama, H. Kawai, T. Morita and T. Sumiyoshi, *J. of Supercritical Fluids*, 2016, **110**, 183.
- H. Sai, L. Xing, J. Xiang, L. Cui, J. Jiao, C. Zhao, Z. Li and F. Li, *J. Mater. Chem. A*, 2013, **1**, 7963.
- D. Wang, E. McLaughlin, R. Pfeffer, Y. S. Lin, *Separation and Purification Technology*, 2012, **99**, 28.
- D. Loche, L. Malfatti, D. Carboni, V. Alzari, A. Mariani and M. F. Casula, *RSC Adv.*, 2016, **6**, 66516.
- M. Alnaief, S. Antonyuk, C. M. Hentzschel, C. S. Leopold, S. Heinrich and I. Smirnova, *Microporous and Mesoporous Materials*, 2012, **160**, 167.
- S. Giray, T. Bai, A. M. Kartal, S. Kizilel and C. Erkey, *Journal of Biomaterial Materials Research Part A*, 2012, **100A**, 1307.
- C. C. Li, Y. T. Chen, Y. T. Lin, S. F. Sie and Y. W. Chen-Yang, *Colloids and Surfaces B: Biointerfaces*, 2014, **115**, 191.
- P. J. Yu, M. H. Lee, H. M. Hsu, H. M. Tsai and Y. W. Chen-Yang, *RSC Adv.*, 2015, **5**, 13985.
- T. Y. Amiri and J. Moghaddas, *International Journal of Hydrogen Energy*, 2015, **40**, 1472.
- C. Buratti and E. Moretti, *Applied Energy*, 2012, **98**, 396.
- Md M. H. Bhuiya, A. M. Anderson, M. K. Carroll, B. A. Bruno, J. L. Ventrella, B. Silberman and B. Keramati, *Ind. Eng. Chem. Res.*, 2016, **55**, 6971.
- M. Tabata, H. Yano, H. Kawai, E. Imai, Y. Kawaguchi, H. Hashimoto and A. Yamagishi, *Orig. Life Evol. Biosph.*, 2015, **45**, 225.
- Y. Wei, J. Wang, Y. Zhang, L. Wang and X. Zhang, *RSC Adv.*, 2015, **5**, 91407-91413.
- H. Ma, A. P. Robert, J. Prévost, R. Jullien, G. W. Scherer, *J. Non-Cryst. Solids*, 2000, **277**, 127.
- A.V. Rao, S. D. Bhagat, H. Hirashima and G. M. Pajonk, *Journal of Colloid and Interface Science*, 2006, **300**, 279.
- J. C. H. Wong, H. Kaymak, S. Brunner and M. M. Koebel, *Microporous and Mesoporous Materials*, 2014, **183**, 23.
- H. Omranpour and S. Motahari, *J. Non-Cryst. Solids*, 2013, **379**, 7.
- R. A. Strøm, Y. Masmoudi, A. Rigacci, G. Petermann, Gullberg L. Chevalier B and M. A. Einarsrud, *J. Sol-Gel Sci. Technol.*, 2007, **41**, 291.
- J. Cai, S. Liu, J. Feng, S. Kimura, M. Wada, S. Kuga and L. Zhang, *Angew. Chem.*, 2012, **124**, 2118.
- A. Fidalgo, J. P. S. Farinha, J. M. G. Martinho, M. E. Rosa and L. M. Ilharco, *Chem. Mater.*, 2007, **19**, 2603.
- M. A. B. Meador, S. L. Vivod, L. McCorkle, D. Quade, R. M. Sullivan, L. J. Ghosn, Nicholas Clark and L. A. Capadona, *J. Mater. Chem.*, 2008, **18**, 1843.
- L. Li, B. Yalcin, B. N. Nguyen, M. A. B. Meador and M. Cakmak, *ACS Applied Materials & Interfaces*, 2009, **1**, 2491.
- H. Maleki, L. Durães and A. Portugal, *J. Mater. Chem. A*, 2015, **3**, 1594.
- Y. Duan, S. C. Jana, A. M. Reinsel, B. Lama and M. P. Espe, *Langmuir*, 2012, **28**, 15362.
- M. A. B. Meador, A. S. Weber, A. Hindi, M. Naumenko, L. McCorkle, D. Quade, S. L. Vivod, G. L. Gould, S. White and K. Deshpande, *ACS Applied Materials & Interfaces*, 2009, **1**, 894.
- K. J. Shea and D. A. Loy, *Chem. Mater.*, 2001, **13**, 3306.
- L. Hu and K. J. Shea, *Chem. Soc. Rev.*, 2011, **40**, 688.
- M. Barczak, P. Borowski, A. Dąbrowski, *Colloids and Surfaces A: Physicochem. Eng. Aspects*, 2009, **347**, 114.
- D. J. Boday, R. J. Stover, B. Muriithi, D. A. Loy, *J. Mater. Sci.*, 2011, **46**, 6371.
- D. J. Boday, R. J. Stover, B. Muriithi, D. A. Loy, *J. Sol-Gel Sci. Technol.*, 2012, **61**, 144.
- Z. Wang, Z. Dai, J. Wu, N. Zhao and J. Xu, *Adv. Mater.*, 2013, **25**, 4494.
- Z. Wang, D. Wang, Z. Qian, J. Guo, H. Dong, N. Zhao and J. Xu, *ACS Appl. Mater. Interfaces*, 2015, **7**, 2016.
- F. Zou, P. Yue, X. Zheng, D. Tang, W. Fu and Z. Li, *J. Mater. Chem. A*, 2016, **4**, 10801.
- M. A. Aegerter, N. Leventis and M. M. Koebel, *Aerogel Handbook*, New York: Springer Science+Business Media, 2011, pp791.

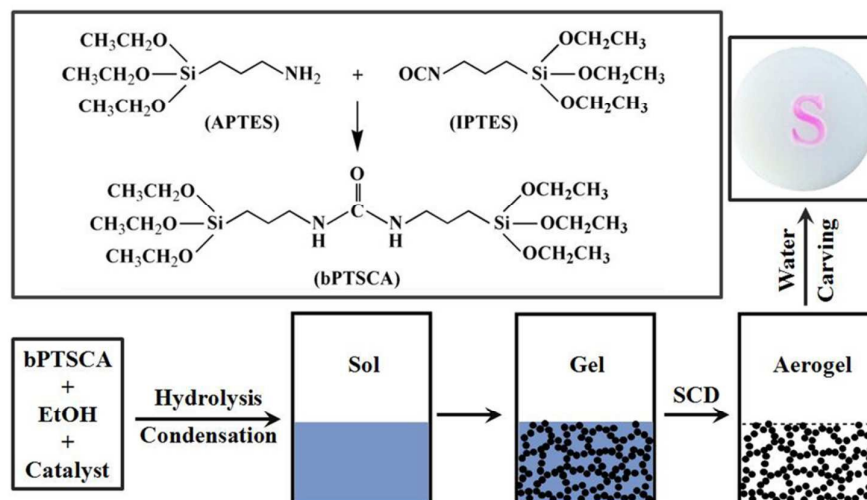
Journal Name

ARTICLE

- 45 C. J. Binker and G. W. Scherer, *Sol-Gel Science: The Physics and Chemistry of Sol-Gel Processing*, San Diego: Academic Press, Inc., 1990, pp108.
- 46 M. Kruk and M. Jaroniec, *Chem. Mater.*, 2001, **13**, 3169.
- 47 G. Zhang, A. Dass, A. M. Rawashdeh, J. Thomas, J. A. Counsil, C. Sotiriou-Leventis, E. F. Fabrizio, F. Ilhan, P. Vassilaras, D. A. Scheiman, L. McCorkle, A. Palczer, J. C. Johnston, M. A. Meador and N. Leventis, *J. Non-Cryst. Solids*, 2004, **350**, 152.

Robust Urethane-Bridged Silica Aerogels Available for Water-Carved Aerosculptures

Yulu Zhang[†], Jin Wang[†], Yong Wei and Xuotong Zhang^{*}



Novel *in situ* bridged silica precursor was used to synthesize robust aerogels for aerosculptures carved with aqueous solvents.